


RESEARCH

Open Access



Astrocytic C–X–C motif chemokine ligand-1 mediates β -amyloid-induced synaptotoxicity

Beatriz G. Perez-Nievas^{1*}, Louisa Johnson¹, Paula Beltran-Lobo¹, Martina M. Hughes¹, Luciana Gammalleri¹, Francesca Tarsitano¹, Monika A. Myszczyńska², Irina Vazquez-Villasenor², Maria Jimenez-Sanchez¹, Claire Troakes¹, Stephen B. Wharton², Laura Ferraiuolo² and Wendy Noble^{1*} 

Abstract

Background: Pathological interactions between β -amyloid (A β) and tau drive synapse loss and cognitive decline in Alzheimer's disease (AD). Reactive astrocytes, displaying altered functions, are also a prominent feature of AD brain. This large and heterogeneous population of cells are increasingly recognised as contributing to early phases of disease. However, the contribution of astrocytes to A β -induced synaptotoxicity in AD is not well understood.

Methods: We stimulated mouse and human astrocytes with conditioned medium containing concentrations and species of human A β that mimic those in human AD brain. Medium from stimulated astrocytes was collected and immunodepleted of A β before being added to naïve rodent or human neuron cultures. A cytokine, identified in unbiased screens of stimulated astrocyte media and in postmortem human AD brain lysates was also applied to neurons, including those pre-treated with a chemokine receptor antagonist. Tau mislocalisation, synaptic markers and dendritic spine numbers were measured in cultured neurons and organotypic brain slice cultures.

Results: We found that conditioned medium from stimulated astrocytes induces exaggerated synaptotoxicity that is recapitulated following spiking of neuron culture medium with recombinant C–X–C motif chemokine ligand-1 (CXCL1), a chemokine upregulated in AD brain. Antagonism of neuronal C–X–C motif chemokine receptor 2 (CXCR2) prevented synaptotoxicity in response to CXCL1 and A β -stimulated astrocyte secretions.

Conclusions: Our data indicate that astrocytes exacerbate the synaptotoxic effects of A β via interactions of astrocytic CXCL1 and neuronal CXCR2 receptors, highlighting this chemokine–receptor pair as a novel target for therapeutic intervention in AD.

Keywords: Astrocyte, Synapse, Beta-amyloid, Alzheimer's disease, CXCL1, Tau

Background

Synapse loss in neocortex and limbic areas is an early pathological feature of Alzheimer's disease (AD) that correlates strongly with cognitive decline [1, 2]. The extent

of synapse loss cannot be fully accounted for by loss of neurons alone, implying that surviving neurons also lose synapses [3, 4]. Loss of connectivity between surviving neurons in AD brain damages the efficiency of neural systems, explaining the association between synapse loss and cognitive decline.

Bioactive soluble dimers, oligomers and to a lesser extent N-terminally extended A β peptides produced by cultured cells, transgenic rodent models of AD, or extracted from human AD brain, reduce dendritic spine number and disrupt synaptic function, long-term

*Correspondence: beatriz.gomez_perez-nievas@kcl.ac.uk; wendy.noble@kcl.ac.uk

¹ Department of Basic and Clinical Neuroscience, Maurice Wohl Clinical Neuroscience Institute, Institute of Psychiatry, Psychology and Neuroscience, King's College London, 5 Cutcombe Road, London SE5 9RX, UK

Full list of author information is available at the end of the article



© The Author(s) 2021. **Open Access** This article is licensed under a Creative Commons Attribution 4.0 International License, which permits use, sharing, adaptation, distribution and reproduction in any medium or format, as long as you give appropriate credit to the original author(s) and the source, provide a link to the Creative Commons licence, and indicate if changes were made. The images or other third party material in this article are included in the article's Creative Commons licence, unless indicated otherwise in a credit line to the material. If material is not included in the article's Creative Commons licence and your intended use is not permitted by statutory regulation or exceeds the permitted use, you will need to obtain permission directly from the copyright holder. To view a copy of this licence, visit <http://creativecommons.org/licenses/by/4.0/>. The Creative Commons Public Domain Dedication waiver (<http://creativecommons.org/publicdomain/zero/1.0/>) applies to the data made available in this article, unless otherwise stated in a credit line to the data.

potentiation and rodent cognition [5–9]. Yet, it remains to be established whether clearance of A β alone is sufficient to prevent synaptic degeneration in AD [10]. Misrouting of modified forms of tau to both the pre-synapse and dendritic spines is also linked with synaptotoxicity in AD [11–14]. We previously reported an association of synaptic tau with dementia in AD. Phosphorylated and oligomeric forms of tau were redistributed from the cytosolic compartment into synaptoneuroosomes in cases with typical AD pathology, synapse loss and dementia, but not in so-called “mismatches” who showed a similar burden of AD pathology but preserved synaptic protein levels and cognition [15]. In addition, we saw increased astrocyte reactivity, as indicated with glial fibrillary acidic protein (GFAP) immunolabelling, in those with AD and dementia relative to mismatch cases [15].

Astrocytes are an intrinsic component of synapses [16] and affect synaptic activity by regulating the availability of glutamate, gamma-aminobutyric acid (GABA), adenosine triphosphate (ATP), and glucose [17–20]. As such, healthy functioning astrocytes are critical for synaptic transmission [21], neural circuit maintenance [22] and long-term potentiation [23].

In AD, and particularly in association with elevated A β or amyloid plaques [24–26], astrocytes become “reactive” leading to changes in their morphology, molecular fingerprint and function [27, 28], and reactive astrocytes are often closely associated with increased disease severity and cognitive decline [29].

However, the specific contribution of reactive astrocytes to AD pathogenesis remains unclear, with some suggesting that reactive astrocytes lose synaptic and neuronal support functions [30] or that astrocytes undergo cellular senescence in AD [31]. Others report neurotoxic effects of reactive astrogliosis, including those mediated by inflammatory astrocytic secretions [32–34]. Particularly in response to repeated insult, systemic or secondary inflammation, astrocytes show exaggerated production and secretion of pro-inflammatory cytokines including interleukin (IL)-1 β , IL-6 and chemokines, such as CXCL1 [35, 36].

Reactive astrocytes may also be neuroprotective, with recent reports showing that astrocytic IL-3 signals to microglia to promote their phagocytosis of aggregated tau and A β [37]. This divergence in astrocytic response may be at least partly related to astrocytic heterogeneity in different brain regions and in response to different types of acute injury [30, 38, 39]. Here, we sought to better understand the contribution of astrocytes to synaptotoxic A β -tau interactions in AD by exposing rodent and human astrocytes to concentrations and species of human A β that replicate those found in human AD brain.

Methods

Postmortem human brain

Post-mortem human prefrontal cortex (Brodmann area 9; BA9) from control and clinically and pathologically confirmed cases of Alzheimer’s disease were obtained from the Neurodegenerative Diseases Brain Bank, King’s College London. Samples were collected from control cases (Braak stage 0, $n=4$) and those with mild AD neuropathology (Braak stages I–II, $n=7$), moderate AD neuropathology (Braak stages III–IV, $n=10$), and severe AD neuropathology (Braak stages V–VI, $n=6$) (Table 1). There were no significant differences in age, gender or post-mortem delay between groups.

Animals

All animal work was conducted in accordance with the UK Animals (Scientific Procedures) Act 1986 and the European Directive 2010/63/EU under UK Home Office Personal and Project Licenses and with agreement from the King’s College London (Denmark Hill) Animal Welfare and Ethical Review Board. Pregnant female CD1 mice purchased from Charles River were used to prepare mouse primary cultures and organotypic brain slices within 5 days of delivery. Tg2576 mice were used to prepare primary neurons that secrete human A β . Tg2576 mice overexpress human APP (isoform 695) containing the double mutation K670N, M671L (Swedish mutation) under the control of the hamster prion protein promoter [40]. Tg2576 mice were originally obtained from Taconic farms (Germantown, NY, USA), and were maintained in-house by breeding males with C57Bl/6/SJL F1 females as recommended by the suppliers. The genotype of the animals was determined by polymerase chain reaction on DNA obtained from the embryos, as previously described [41]. Water and food were available (Picolab rodent diet 20; # 5053; Lab Diet, St Louis, MO, USA) ad libitum. Animals were housed at 19–22 °C, humidity 55%, 12-h:12-h light:dark cycle with lights on at 07:30.

Mouse primary neural cell cultures

To obtain A β -containing medium (transgenic conditioned media or TGCM), we prepared primary neurons from the cerebral cortex of Tg2576 mice at embryonic day 15, as previously described [42]. Neurons were plated at a density of 6×10^5 viable cells/35mm² on glass-bottomed dishes (MatTek Corporation, Ashland, MA, USA), 96-well plates (BD Falcon) or 12-well Nunc[™] plates (ThermoFisher Scientific) previously coated with PDL (10 μ g/ml) for at least 1 h at 37 °C. Cultures were maintained at 37 °C in 5% CO₂, in neurobasal medium with 2% B27 nutrient, Glutamax, penicillin (100 units/ml) and streptomycin (100 μ g/ml). After 14 DIV medium from healthy neurons was collected [43]. Media collected

Table 1 Human postmortem samples from BA9 prefrontal cortex, that were used in this study

Sex	Age (Y)	PMD (h)	Braak stage	ApoE	Observations
M	59	50	0	n/a	Normal adult brain
M	40	40	0	n/a	Normal adult brain
M	78	10	0	2/3	Ageing changes (mild)
F	82	13	0	2/3	Argyrophilic grains low to moderate density
F	92	17	I	3/3	Control brain with some tau deposition
F	55	12	I	n/a	Minimal tau pathology consistent with HP-tau stage-I
F	81	17	I	3/3	Mild ageing changes Braak I
M	81	18	I	n/a	control—old cerebral infarct (Braak I)
M	93	33	II	3/3	Mild alzheimer-type changes—Braak II
F	84	35	II	n/a	Alzheimer changes Braak II consistent with normal ageing
F	97	39	II	n/a	Very mild Alzheimer's disease type changes BNE stage 2, control
M	92	11	III	n/a	Mild alzheimer-type changes—Braak III
F	70	38	III	n/a	Possible AD (CERAD) Braak III (limbic) BNE stage III
M	86	52	III	n/a	Alzheimer type changes (ageing), BNE stage 2, control
F	98	3.5	III	n/a	Alzheimer's disease BNE IV, CERAD probable; TDP-43 pathology (hippocampus and amygdala)
F	89	36.5	III	3/3	Alzheimer's disease pathology (BNE stage IV) with amyloid angiopathy & limbic TDP-43 pathology but cognitively not impaired
M	82	28	IV	n/a	AD (modified Braak IV) with limbic TDP-43 pathology
M	86	53	IV	n/a	AD (modified Braak IV) with extensive severe amyloid angiopathy
F	83	22	IV	n/a	AD (limbic stage-modified Braak IV) with moderate–severe amyloid angiopathy
F	89	56	IV	n/a	AD HP tau stage 4, severely affecting limbic system and moderately extending to neocortex
M	92	70	IV	n/a	Alzheimer's disease (BNE stage 4)
F	80	13	V	3/4	AD Braak V with mild amyloid angiopathy
M	86	26	V	4/4	AD Braak V with moderate amyloid angiopathy
F	84	24	V	4/4	Alzheimer's disease Braak 5
F	97	12	V	3/3	Alzheimer's disease Braak V
M	72	5	VI	3/3	AD Braak VI with marked amyloid angiopathy
F	91	28.5	VI	3/4	Alzheimer's disease, Braak VI

Age is shown in years (y), postmortem delay (PMD) in hours (h), sex, ApoE genotype (when known) and Braak stage. Braak stage 0 cases had some phospho-tau but did not meet Braak stage I criteria and were used as controls

from 14 DIV wild-type neurons cultured from littermates (wild type conditioned media or WTCM) was used as a control.

Primary neurons were obtained from cerebral cortex of CD1 embryos as described above. Neurons were transfected at 5–7 DIV with the plasmid pEGFP-N1 (Clontech, Mountain View, CA) using lipofectamine 2000 (ThermoFisher Scientific).

Primary astrocytic cultures were prepared from the cortex of wild type CD1 mice on postnatal days 1–3 as previously described [44]. The astrocytes were seeded onto a poly-D-lysine (PDL 10 µg/ml) precoated T75 flasks and maintained in culture for 7–10 days in a humidified CO₂ incubator at 37 °C with shaking at 200 rpm overnight on days 3 and 7 to remove remaining microglia and oligodendrocytes. Astrocyte-enriched cultures were trypsinized using TrypLE (ThermoFisher Scientific) and replated on PDL precoated 6- or 12-wells plates until they reached 13–14 DIV. 24 h before treatment (as

described below), growth medium (high glucose DMEM with glutamax, 10% fetal bovine serum, 100 units/ml penicillin and 100 µg/ml streptomycin) was changed to Neurobasal-B27 serum-free medium.

For co-culture experiments, primary astrocytes were plated on cell-culture inserts (0.4 µm pore membrane, Falcon, Corning, Corning, NY, USA) that allow the passage of small molecules between cells and culture medium, and neurons were plated on 6 well plates, as described above. Astrocytes were treated with TGCM or WTCM for 24 h, the medium was removed (TGCM astro and WTCM astro), the cells washed with PBS and inserts placed on top of cultured neurons for another 24 h. There was no direct contact between neurons and astrocytes.

Human astrocyte and neuronal cell cultures

Skin fibroblasts from three control subjects were used (Table 2). These were reprogrammed as previously described [45]. Once induced, neuronal progenitor

Table 2 Characteristics of human donors from whom fibroblasts were obtained

Line ID	Type	Sex	Age	Ethnicity
155	Control	M	40	Caucasian
209	Control	F	69	Caucasian
3050	Control	M	65	Caucasian

Line ID, type (disease or control), sex, age in years and ethnicity are shown

cells (iNPC) cultures were established, and the medium was switched to NPC proliferation media consisting of DMEM/F12 (1:1) GlutaMax, 1% N2, 1% B27, and 40 ng/ml FGF2. iNPC-derived astrocytes were produced as previously described [45–47]. Briefly, iNPCs were switched to astrocyte proliferation media, DMEM (Thermo Fisher Scientific), 10% FBS (Life science production, Bedford, UK), 0.2% N2 (Thermo Fisher Scientific). Cells were differentiated in 6-well plates coated with human fibronectin for 7 days and were used at a matched number of passages.

Lund human mesencephalic (LUHMES) neuronal precursors were grown in T75 flasks in proliferation medium DMEM/F12 GlutaMAX™ supplement medium (Thermo Fisher Scientific), N2 supplement (Thermo Fisher Scientific) and 40 ng/ml recombinant basic fibroblast growth factor (FGF) (Peprotech). To allow high content imaging on the Opera Phenix microscope, non-differentiated LUHMES were transduced with GFP-expressing lentiviral particles (LV-GFP), with GFP expression under the control of a PGK promoter as previously described [48]. When cells were 50–60% confluent they were differentiated by adding differentiation media consisting of DMEM/F12 GlutaMAX™ supplement medium, N2 supplement and 1 µg/ml tetracycline. After 2 days, LUHMES were trypsinized and replated onto 96 wells plates for a further 3 days before experimentation.

Mouse organotypic brain slice culture

Organotypic brain slice cultures were prepared from P9 wild-type CD1 mice and cultured as described in Croft et al. [49]. Briefly, pups were culled by decapitation in accordance with the UK Animals in Scientific Procedures Act (1986). Brains from pups were bisected into hemi-brains by a single cut along the midline. The cerebellum, thalamus and brainstem were removed and discarded to leave the cortex, hippocampus and connecting areas. These were kept in ice-cold dissection buffer [1.25 mM KH₂PO₄ pH 7.4, 124 mM NaCl, 3 mM KCl, 8.19 mM MgSO₄, 2.65 mM CaCl₂, 3.5 mM NaHCO₃, 10 mM glucose, 2 mM ascorbic acid, 39.4 µM ATP in ultrapure H₂O, sterile filtered (0.2 µm)] with constant oxygenation throughout the preparation procedure. 350 µm coronal slices were cut using a McIlwain Tissue

Chopper (Stoelting Europe, Ireland). Eighteen slices from each hemi-brain were collected and 3 consecutive slices per well were positioned on interface-style Millicell culture inserts (Millipore (UK) Ltd.) in 6 well culture plates (ThermoFisher Scientific, UK) containing 1 mL of sterile slice culture medium (Basal medium eagle (BME), 1 mM HEPES, pH 7.1, 19.3 mM NaCl, 5 mM NaHCO₃, 511 µM ascorbic acid, 40 mM glucose, 2.7 mM CaCl₂, 2.5 mM MgSO₄, 1% (v/v) GlutaMAX (Life Technologies, Paisley, UK), 0.033% (v/v) insulin, 0.5% (v/v) penicillin/streptomycin (Life Technologies), in ultrapure H₂O, sterile filtered (0.2 µm), plus 25% (v/v) heat inactivated horse serum (ThermoFisher, UK). Three hours after plating, the culture medium was removed by aspiration and replaced with 1 ml of pre-warmed fresh sterile culture medium. Brain slices were incubated at 37 °C and the culture medium was changed from the bottom of each well every 2–3 days. Slices were maintained for a minimum of 14 day in vitro prior to treatment with WTCM or TGCM as described below.

Cell and slice culture treatments

To treat cells and slice cultures with concentrations and species of Aβ that mimic those in human AD brain, we collected the medium from cultured Tg2576 neurons. Aβ in this culture medium is naturally secreted at a 10:1 ratio of Aβ₄₀:Aβ₄₂. The concentration of Aβ in TGCM was determined by ELISA (ThermoFisher Scientific) following the manufacturer's instructions. To mimic Aβ levels in human AD brain [50], medium was diluted (in culture medium) to reach 2000 pM Aβ₄₀/200 pM Aβ₄₂, as described previously [42, 50–52]. An equivalent volume of WTCM was used as control. TGCM or WTCM was added directly to the culture medium of mouse or human astrocyte or neuron cultures, or directly on top of mouse organotypic brain slice cultures, for 24 or 48 h.

To test the direct effects of the cytokine CXCL1 on synapse/neuronal health, DIV12–13 neurons were pre-treated for 20 min with 40 ng/ml of an antagonist of the CXCL1 receptor in neurons, CXCR2 (SB225002, Tocris Bioscience), prior to the addition of 40 nM recombinant mouse CXCL1 (R&D Systems) or vehicle for a further 24 h.

Immunodepletion of Aβ

To remove Aβ from the medium of astrocytes challenged with TGCM prior to application of astrocyte conditioned medium to neurons, immunodepletion was used, as previously described [50]. Briefly, 24 h after treatment of astrocytes with TGCM, medium was collected and incubated with protein G Dynabeads (ThermoFisher) bound with 9 µg of 6E10 antibody (COVANACE) for 90 min at 4 °C, according to the manufacturer and previously

published protocols [50]. Beads were separated from medium using a magnetic stand to remove A β -6E10 complexes. The efficacy of immunodepletion was assessed by measuring levels of A β before and after 6E10 immunodepletion by ELISA and western blot (Additional file 1: Fig. S1A, B).

Isolation of synaptoneurosomes and analysis of protein content in each fraction

Total, cytosolic and synaptic fractions were isolated from human brain tissues or mouse organotypic brain slice cultures as previously described [15, 53]. Briefly, synaptoneurosomes were prepared from ~ 250 mg of frozen tissue (grey matter) or from three pooled wells (9 consecutive slices) of slice cultures. Tissue was homogenized in 1.5 ml or 250 μ l of ice-cold Buffer A (25 mM HEPES, pH 7.9, 120 mM NaCl, 5 mM KCl, 1 mM MgCl₂, 2 mM CaCl₂, 1 mM dithiothreitol, protease inhibitors, phosphatase inhibitors) for brain tissue or slices, respectively, using a Teflon-glass mechanical tissue grinder at 170 rpm and filtered through 80 μ m pore filters. A portion of the filtrate was collected, supplemented with 1.5% SDS, boiled for 5 min, and centrifuged at 15 000 *g* for 15 min, to give the total protein fraction. The remaining sample was filtered through 5 μ m pore filters and centrifuged at 1000 *g* for 10 min to pellet synaptoneurosomes. The supernatant was collected as cytosolic extract, which was further centrifuged at 100, 000 *g* for 30 min to remove microsomes. The synaptoneurosomes pellet was washed once with cold Buffer A and centrifuged again at 1000 *g* for 10 min. The pellet was extracted with Buffer B (50 mM Tris pH 7.5, 1.5% SDS, 2 mM dithiothreitol) (0.5 ml for human brain, 80 μ l for slices) and boiled for 5 min. After centrifugation at 15,000 *g* for 15 min, the supernatant was collected as the synaptoneurosomes fraction.

Protein concentrations in each fraction were determined using a bicinchoninic acid (BCA) protein concentration assay kit (Pierce) according to the manufacturer's instructions and were adjusted to the same concentration for all fractions by adding homogenisation buffer. Tau content in total, cytosolic and synaptoneurosomal fractions was examined for organotypic brain slice culture experiments. The cytosolic fraction of postmortem human brain was used for cytokine arrays.

Cytokine arrays

The cytoplasmic fraction of human postmortem brain homogenates and astrocyte culture media were used to determine cytokine content using Mouse or Human Proteome Profiler arrays (Mouse Cytokine Array Panel A and Human Cytokine Array, R&D Systems), according to the manufacturers' instructions. Positive and negative control spots included were used to allow quantitative

analysis of cytokine levels. Results were expressed as percentage change compared to controls.

SDS-PAGE and western blotting

To collect a total protein fraction of cultured cells for SDS-PAGE and western blot, cultured cells were washed with PBS to remove medium and were directly lysed into PBS containing sample buffer (NuPAGE LDS Sample Buffer 4X, Invitrogen), reducing agent (NuPAGE Sample Reducing Agent 10X, Invitrogen), protease inhibitor (complete Mini EDTA-Free Protease Inhibitor Cocktail, Roche, Basel, CH) and phosphatase inhibitor (PhosSTOP, Roche) cocktails.

Equal protein amounts were separated on 10% or 4–12% SDS-PAGE gels (Thermo Fisher Scientific) by electrophoresis, transferred to 0.45 μ m nitrocellulose membranes (Millipore, MA, USA), and immunoblotted as described previously (Glennon et al. 2020). Primary antibodies were against PSD-95 (Rabbit IgG, #3409, Cell Signalling 1/500), synapsin-1 (Rabbit IgG, #BV-6008, Enzo 1/500), caspase-3 (Rabbit IgG, #9661, Cell Signalling 1/500), GFAP (Mouse IgG, Z0334, DAKO Ltd, 1/500), phosphoNF κ B (Rabbit IgG, #3031, Cell Signalling, 1/1000), β -amyloid-6E10 (Mouse IgG, SIG-39320, 1/200–1/500), lipocalin-2/NGAL (Mouse IgG, #AF1857, 1/500), tau (Rabbit IgG, #A0024, DAKO Ltd, 1/5000), PHF1 (Mouse IgG, P. Davies, 1/2000), GAPDH (Mouse IgG, #32233, SantaCruz Biotechnology, 1/500), β -actin (Mouse IgG, #ab8226, 1/1000), α -tubulin (Rabbit IgG, #ab18251, 1/1000). Bound antibodies were imaged using an Odyssey CLX instrument (LI-COR Biosciences) and band intensities were quantified using the Image Studio Software (LI-COR Biosciences). For analysis of synaptic proteins and markers of astrocyte reactivity, the band intensity of the protein of interest was normalised to that of a loading control (β -actin or GAPDH) in the same sample. For western blots of synaptoneurosomes, the amount of total tau or phosphorylated tau in the synaptoneurosomes fraction was normalised to the amount of total tau or phosphorylated tau in the cytosolic fraction of the same sample. Data is shown as % average control, with the control for each experiment stated in the figure legend.

Immunocytochemistry

Cells were fixed for 10 min in 4% paraformaldehyde and 4% sucrose in PBS and then for 10 min in pre-chilled methanol. Cells were simultaneously permeabilized and blocked using PBS containing 2% normal goat serum and 0.1% Triton-X-100 for 1 h at room temperature. Immunolabelling was performed according to previously published protocols [54]. Primary antibodies were against tau (Rabbit IgG, #A0024, DAKO, 1/500), MAP2 (Mouse IgG,

#GTX8266, GeneTex, 1/200), and GFAP (Rabbit IgG, #Z0334, DAKO, 1/100), and the appropriate species of AlexaFluor-conjugated secondary antibodies (Goat anti-rabbit IgG or Goat anti-mouse IgG, Life Technologies). High-resolution digital images were acquired using the Opera Phenix High Content Screening System in confocal mode with a Zeiss 20× water NA 1.0 objective. The fluorophores were detected with the following excitation and emission (Ex/Em) wavelengths: Hoechst 33342 (405/435–480), AF488 (488/500–550), and far red (wavelengths above 655 nm). Cell segmentation and quantification analyses were performed using the Harmony software, version 4.9. The experimenter was blinded to treatment.

Measurement of dendritic spine density, neuron complexity and tau mislocalisation

For the analysis of dendritic spine structure and neuronal complexity, neurons at 14 DIV were transfected with the plasmid peGFP-N1 (Clontech, Mountain View, CA) using Lipofectamine 2000, fixed 24 h post-transfection, and the GFP-expressing cells were imaged using high-resolution confocal digital images obtained from an Opera-Phenix microscope (Perkin-Elmer) as described above. NeuronStudio software (CNIC, Mount Sinai School of Medicine) was used for dendritic spine analysis. Dendritic spine densities were calculated from approximately 20 neurons/condition for each biological replicate. Spine density, or number of neuritic protrusions was defined as number per micrometer of dendrite/neurite length. The experimenter was blinded to treatment.

Neuronal complexity was analysed as a measure of neuron health using Harmony software which gives automated (therefore, blinded) measures of mean and maximum neurite length, number of roots (number of junctions of neurites with the cell body), nodes (number of neurite branch points), segments (total number of individual branches) and extremities (number of distinct neurite ends). A reduction in neurite number or in complexity measures is indicative of reduced neuronal health [34]. The number of neurites per cell containing mis-sorted tau was assessed with Harmony™ software using an algorithm that identifies neurite segments (labelled with MAP2) that contain tau.

Statistical analysis

Data were analysed using GraphPad Prism. After performing a Shapiro–Wilk normality test, most data were analysed using one-way ANOVA followed by Tukey post hoc test or Student's *t* test (GraphPad Prism 7 Software, Graphpad Software, La Jolla, CA, USA). Results were considered statistically significant when $p < 0.05$. For neurons treated with astrocyte conditioned media and the

CXCR2 antagonist, a two-way ANOVA followed by post hoc tests was performed (see figure legends). Data are shown as mean \pm standard error of the mean (SEM).

Results

Conditioned medium from A β stimulated astrocytes is synaptotoxic

Primary neurons cultured from Tg2576 mice release human A β into the culture medium in an approximately 1:10 ratio of A β 42:A β 40 as in human AD brain (Wu et al., 2010). Here, conditioned medium was collected from primary cortical neurons from wild-type or Tg2576 mice (WTCM; TGCM), diluted in neurobasal medium to human brain levels (200 pM A β 42, 2000 pM A β 40; [50]) and applied to astrocytes or neurons. The conditioned medium from stimulated astrocytes was collected, (WTCM astro and TGCM astro) and in some experiments A β was immunodepleted from the medium of TGCM treated astrocytes (TGCM astro-ID). These media were added to naïve WT primary neurons. Direct exposure of naïve neurons to TGCM induces a decrease in the number of dendritic spines compared to neurons treated with medium from wild type littermates (WTCM) [42, 51, 52]. This finding was reproduced here (Fig. 1A) with spine numbers in TGCM-stimulated neurons being reduced by approximately 36% to $66.42 \pm 6.233\%$ relative to WTCM conditions ($p < 0.001$). Notably, spine loss was exacerbated (reduction of 51.60 ± 5.26 SEM% relative to WTCM) when neurons were exposed to medium from astrocytes stimulated with TGCM (TGCM astro) compared to those treated with WTCM (WTCM astro). Importantly, this effect is still observed after immunodepleting A β from the medium using 6E10 (TGCM astro-ID) (Fig. 1A, B; Additional file 1: Fig. S1), demonstrating that soluble factors released by astrocytes mediate this heightened synaptotoxicity.

A reduction in the levels of synaptic proteins including PSD95 and synapsin-1 was found in neurons exposed to medium from TGCM-stimulated astrocytes compared to medium from WTCM treated astrocytes (Fig. 1C–E). This was accompanied by increases in levels of cleaved (active) caspase-3 (Fig. 1C, F), an executioner caspase which also plays various non-apoptotic roles in neurons including in proteolysis and modulation of synaptic functions [55]. The changes in synaptic proteins and cleaved caspase-3 are induced by astrocytic secretions, since they are still observed after A β is immunodepleted from the astrocyte-conditioned TGCM (TGCM astro-ID; Fig. 1D–F). Please note that the difference in cleaved caspase-3 between WTCM and TGCM-ID was not significant, as a result of slightly higher levels of variation in the TGCM-ID data (Mean \pm SEM: WTCM astro 100 ± 2.496 ; TGCM astro 121.2 ± 11.08 ; TGCM astro ID

120.1 ± 13.86). Similarly, neurons treated with medium from TGCM-stimulated astrocytes showed indicators of poor health shown by reduced neuronal complexity measures (Fig. 1G) including significant reductions in total neurite length and number of roots, alongside non-significant decreases in other parameters that measure neuritic ramification (Fig. 1H, J; Additional file 1: Fig. S2).

To validate this data in more physiological co-culture conditions, astrocytes were grown on cell culture inserts and stimulated with TGCM or WTCM. The culture medium was replaced to remove traces of A β and the stimulated astrocytes co-cultured with neurons (Fig. 1K). Under these conditions, astrocytic secretions were also found to disrupt synapses indicated by significantly reduced PSD-95 ($p < 0.05$), apparent (but non-significant) reductions in synapsin-1 levels, and significant increases in cleaved caspase-3 ($p < 0.05$) (Fig. 1K–M) in the absence of elevated lactate dehydrogenase (LDH) release (Additional file 1: Fig. S2B). This confirms that factors released by astrocytes in response to concentrations of human A β , similar to that found in AD brain, compromise synaptic and neuronal health without causing overt neurotoxicity.

Despite recent studies indicating significant conservation between human and mouse astrocytes, there are species-specific differences in their response to stressors [56]. Therefore, human iNPC-astrocytes, which retain age-related features [57], were stimulated with TGCM or WTCM, the astrocyte conditioned medium collected and immunodepleted of A β with 6E10, prior to its addition to human post-mitotic neurons that were differentiated from LUHMES cells. LUHMES are a fetal human mesencephalic cell line conditionally immortalised with a myc transgene which become post-mitotic mature neurons when transgene expression is suppressed [58] and that have utility for high throughput

screening of neuronal morphology [59]. Similar to findings with mouse cells, medium from TGCM-exposed human astrocytes (TGCM h-astro) induced a significant loss of neuritic protrusions (Fig. 2A, B, $p < 0.001$) and reductions in features of neuronal health and complexity, measured in cells containing axons, relative to WTCM h-astro ($p < 0.05$, Fig. 2C, D; Additional file 1: Fig. S3), that were retained in the absence of A β (TGCM h-astro-ID, $p < 0.05$ for all).

Astrocyte-mediated synaptotoxicity in response to A β is related to tau mislocalisation

Direct effects of A β on synapse and neuron health are tau-dependent [11, 57] and related to damaging effects of mislocalised tau at post-synapses [11, 12] and pre-synapses [13, 14]. We found that tau localisation was altered in response to medium from TGCM astro, with tau showing increased neuritic localisation as indicated by elevated numbers of MAP2-positive neurites (green) containing tau (far red) (Fig. 3A, B). Similar findings were observed when organotypic brain slice cultures which contain all neural cell types, were treated with TGCM. Synaptoneurosome fractionations were used to yield cytosolic and synaptic fractions. Western blotting of these samples showed that tau is present in the cytosolic fraction and appears enriched in the synaptic fraction of slices treated with WTCM and TGCM. Quantification of the amount of synaptoneurosome tau relative to tau in the cytosolic fraction of the same sample, as is standard for this type of analysis [15, 53] showed that in slices treated with TGCM the ratio of synaptic to cytosolic tau phosphorylated at Ser396/404 (PHF1) is increased when compared to slices treated with WTCM (Fig. 3C–E).

(See figure on next page.)

Fig. 1 Conditioned medium from A β -stimulated astrocytes exaggerates the damaging effects of A β at synapses. **A** Dendritic spine density was measured in neurons transfected at 7DIV with GFP and treated with WTCM astro, TGCM astro and TGCM astro-ID or directly with WTCM and TGCM at 13DIV for 24 h. Representative images are shown. Scale bar is 10 μ m. **B** Quantification of spine density in 10–20 neurons per experimental replicate from eight individual neuron preps ($n = 8$). TGCM astro caused increased dendritic spine loss relative to treatment with TGCM directly, and this is maintained when A β is immunodepleted from the medium. Box indicates data from neurons directly exposed to TGCM or WTCM for clarity. Data was analysed by ordinary one-way ANOVA and Tukey's post-hoc tests. **C** Neuronal lysates were immunoblotted using antibodies against PSD-95 (95 kDa), synapsin-1 (77 kDa), cleaved caspase-3 (17–19 kDa) and β -actin (42 kDa). Representative blots are shown. Western blot band intensities were quantified and showed that TGCM astro caused reductions in the abundance of the synaptic markers **D** PSD-95 and **E** synapsin-1 and an increase in **F** cleaved (active) caspase-3, that is maintained when A β was immunodepleted (TGCM astro-ID). Data is from eight individual neuron preps ($n = 8$), each of which have two experimental replicates. Data was analysed by ordinary one-way ANOVA and Tukey's multiple comparison post-hoc tests. **G** Neuronal complexity as a measure of neuron health was analysed for all cells in three wells of five biological replicates ($n = 5$) using Harmony software. This showed **H** reduced total neurite length, and fewer number of **I** nodes and **J** roots following treatment with TGCM astro and TGCM astro-ID, indicating that astrocytic secretions are damaging to neurons. Data was analysed by ordinary one-way ANOVA and Tukey's multiple comparison post-hoc tests. **K** Astrocytes were cultured and treated in cell culture inserts, the medium removed by washing and the astrocytes added to neuron cultures. Representative western blots of neuronal lysate from co-culture experiments are shown. Western blot data was quantified by normalising the protein of interest to β -actin levels in the same sample and showed reduced **L** PSD-95 and **M** synapsin-1, and **N** increased levels of cleaved caspase-3 when neurons were co-cultured with astrocytes that had previously been exposed to TGCM ($n = 6$, data is from six independent experiments, each of which had three technical replicates). Data was analysed using an unpaired t test. Data on graphs is mean \pm SEM and is shown as percentage average control (WTCM astro). * $p < 0.05$, ** $p < 0.01$

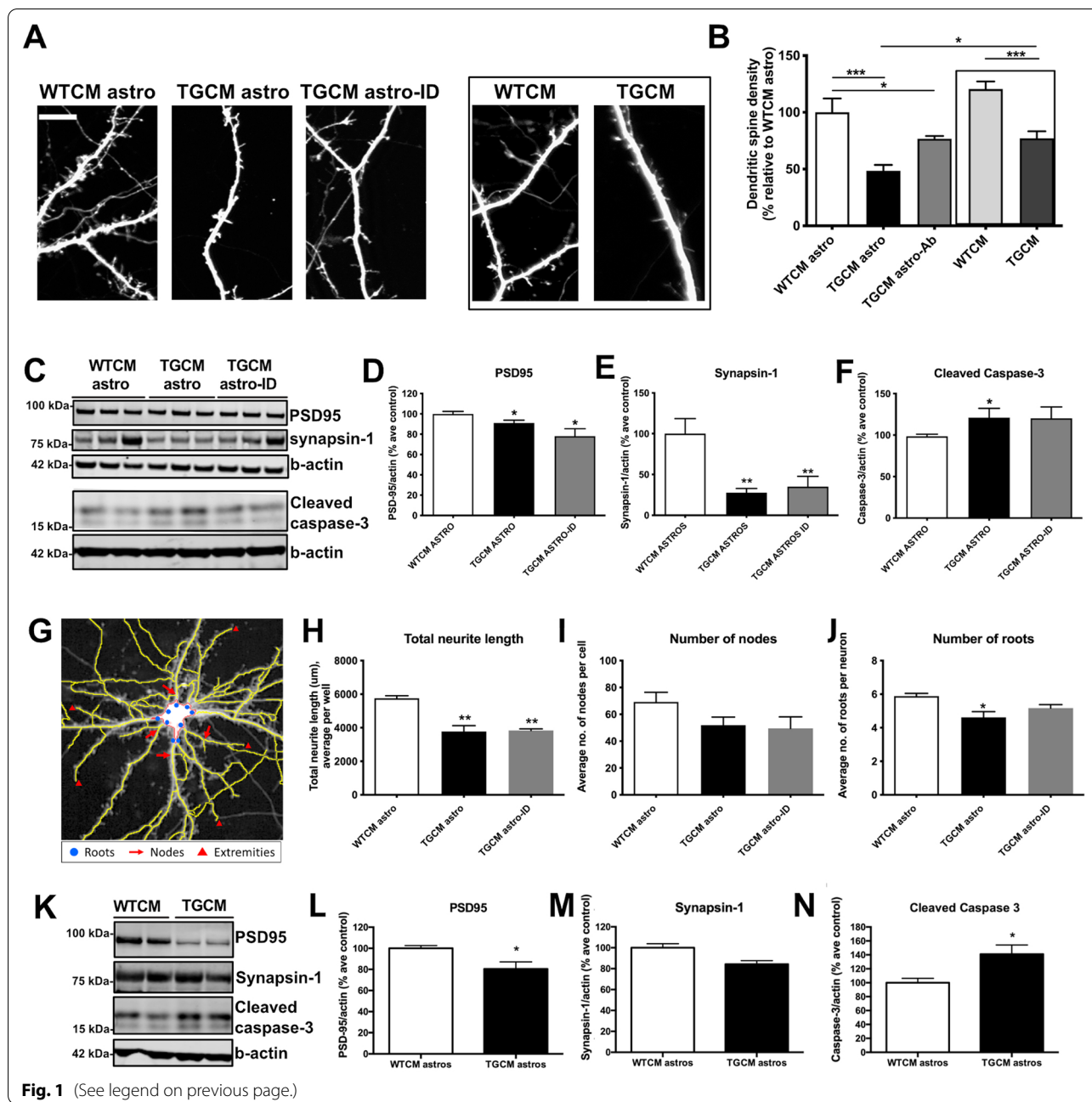
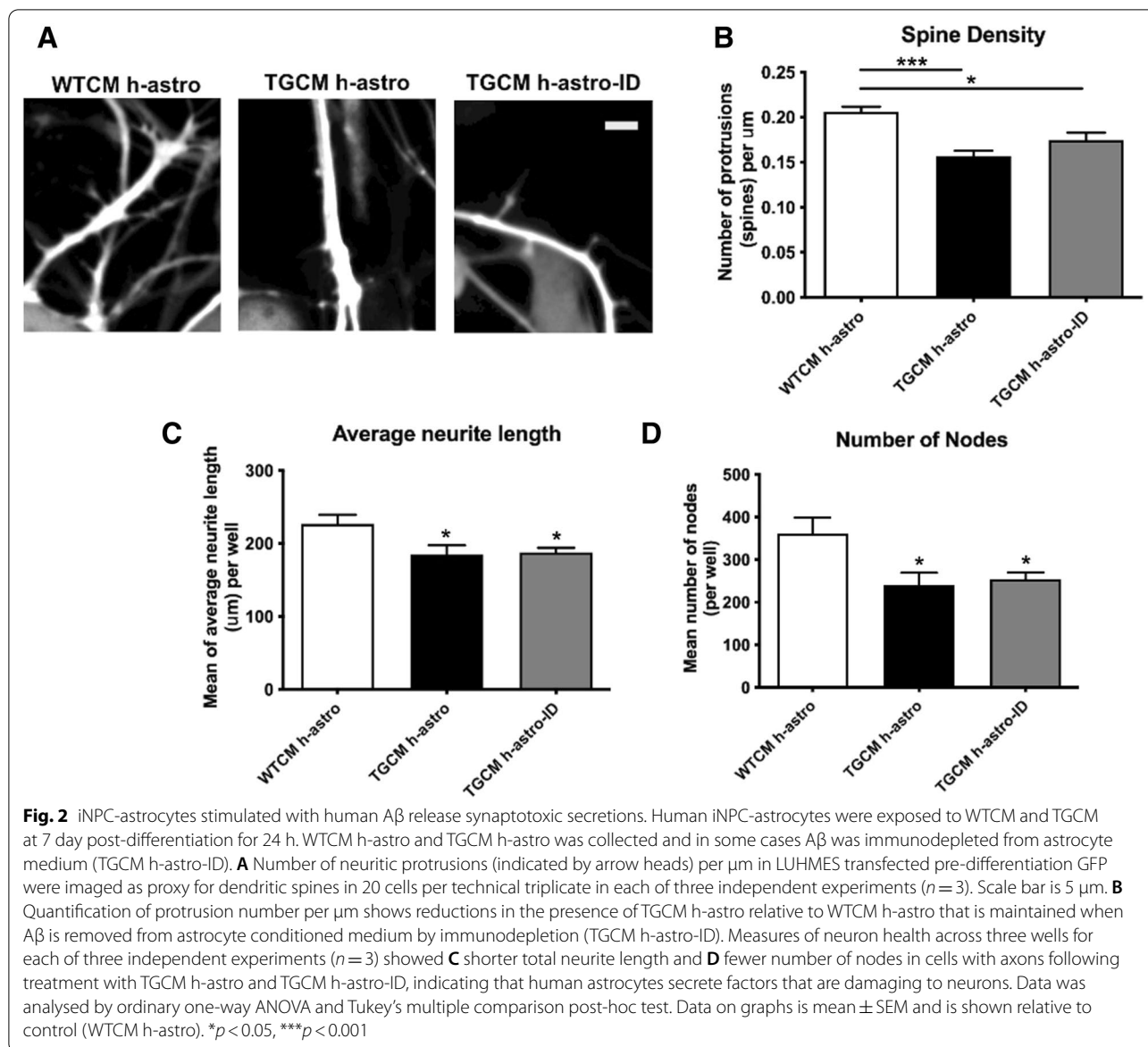


Fig. 1 (See legend on previous page.)

Astrocytic inflammatory phenotypes are induced by Aβ

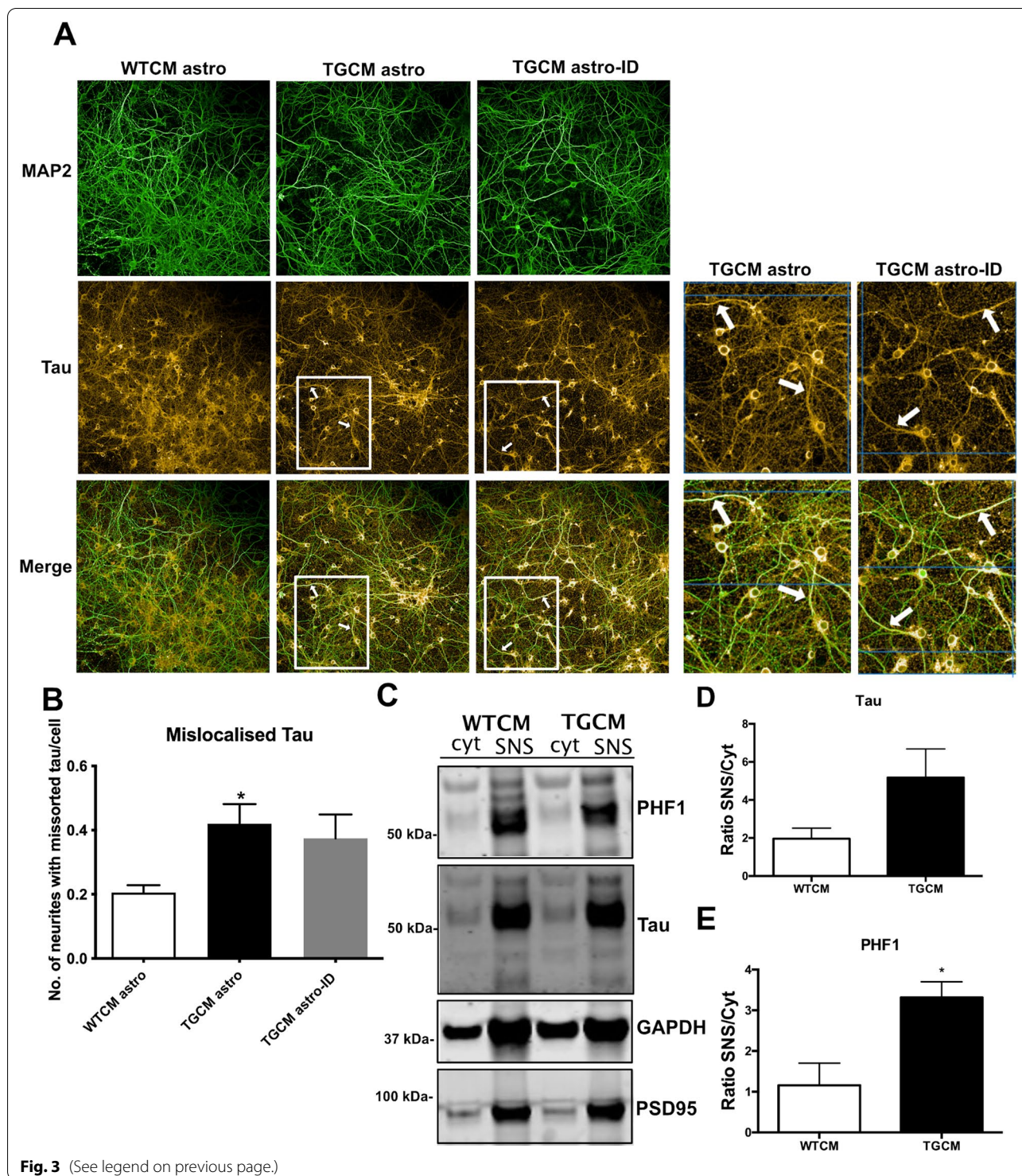
Although microglia are considered the resident immune cell in the brain, the contribution of astrocytes to neuroinflammatory processes in AD is increasingly recognised [25, 35, 36]. We observed increased levels of GFAP, and other markers of astrocyte reactivity including lipocalin-2 (Lcn2), in astrocytes stimulated with TGCM relative to WTCM (Fig. 4A–G). Lcn2 was identified as a pan-reactive astrocyte marker in gene expression analyses [38] and we previously showed significant

elevations in astrocytic lcn2 levels upon their exposure to oxysterol mixtures that mimic their composition in AD brain [34]. These changes reflect the induction of inflammatory signalling pathways in astrocytes, since we observed increased phosphorylation of NFκB (p65) upon exposure of astrocytes to Aβ-containing medium relative to control (WTCM) conditions (Fig. 4C, F). We examined cytokine release from astrocytes using cytokine arrays which allowed unbiased measurement of a panel of cytokines and chemokines in astrocyte



(See figure on next page.)

Fig. 3 Astrocyte-mediated synaptotoxicity in response to Aβ is accompanied by tau mislocalisation. **A** 14DIV neurons treated for 24 h with WTCM astro, TGCM astro or TGCM astro-ID were fixed and immunolabelled with antibodies against MAP2 (green) and tau (far red). Exposure to TGCM astro and TGCM astro-ID induced increased tau localisation in neurites with white arrows indicating beading of these neurites. Scale bar is 100 μm (20 μm in inset). **B** The number of MAP2 labelled neurites per cell containing missorted tau was quantified, showing increased tau mislocalisation upon exposure to conditioned medium from astrocytes exposed to Aβ (TGCM astro and TGCM astro-ID) (n = 4, four independent experiments each performed in triplicate). Data was analysed by ordinary one-way ANOVA and Tukey's multiple comparison post-hoc test, and is shown relative to control (WTCM astro). **C** To confirm that Aβ induces tau mislocalisation in the presence of other neural cell types, 14DIV organotypic brain slice cultures prepared from CD1 mice were treated with WTCM or TGCM for 24 h. The cytosolic fraction (Cyt) and synaptoneurosomes (SNS) were extracted and immunoblotted with antibodies against PSD-95, total tau and tau phosphorylated at Ser396/404 (PHF1). GAPDH was used as a loading control. PSD-95 accumulates in the synaptic fraction showing successful SNS extraction. The abundance of **D** tau and **E** PHF1 in synaptoneurosomes relative to the amount of tau or PHF1 in the cytosolic fraction of the same sample was determined. Phosphorylated tau showed increased synaptic localisation following exposure to TGCM (n = 3, three independent slice culture preparations from which three wells of each were pooled). Data was analysed using unpaired t tests. Data on graphs is mean ± SEM and is shown relative to vehicle control. *p < 0.05



conditioned medium. This showed upregulation of a small number of cytokines including CXCL1, M-CSF and CCL2 in medium from TGCM-treated mouse primary astrocytes relative to WTCM treated cells (Fig. 4H, I), and CXCL1 and IP-10 from TGCM-treated

iNPC-astro (Fig. 4J, K). Aβ-containing medium significantly increased the secretion of CXCL1 from both mouse and human astrocytes (Fig. 4I, K). Notably, CXCL1 levels are increased in AD brain homogenate relative to samples from age-matched controls (Fig. 4L,

M), and CXCL1 has previously been implicated in AD-associated tau changes [60].

CXCL1 is synaptotoxic

To determine if the synaptotoxic effects of culture medium from TGCM-stimulated astrocytes is mediated by CXCL1, we applied recombinant CXCL1 to primary neurons. This significantly reduced spine number by $66.56 \pm 9.89\%$ (Fig. 5A, B), similar to the reductions identified previously using whole TGCM astro. Measures of neuron health including neurite length and number of nodes and roots were also affected by recombinant CXCL1 (Fig. 5C–E). CXCL1-mediated synaptotoxicity was prevented when neurons were pre-treated with an antagonist (SB225) of the CXCL1 receptor, CXCR2 (Fig. 5A–E, Fig. S4). These results strongly implicate CXCL1 in the synaptotoxic effects of astrocytes in response to physiological concentrations of human A β .

CXCL1–CXCR2 interactions mediate the A β -induced synaptotoxic responses of astrocytes

Finally, we determined that blocking the CXCR2 receptor is sufficient to prevent synaptotoxicity in response to secretions from A β -stimulated astrocytes. Here, astrocytes were stimulated with TGCM or WTCM as before, and the astrocyte conditioned medium was applied to primary neurons that had been pre-incubated with the CXCR2 antagonist SB225. Blocking the CXCL1 receptor prevented the reductions in spine density (Fig. 6A, B) and measures of neuron complexity (Fig. 6C–E) that resulted from A β -stimulated astrocyte medium (TGCM astro). These data strongly implicate CXCL1–CXCR2 interactions in the synaptotoxic effects of astrocytes in response to AD-mimicking concentrations of human A β .

Discussion

It is now established that non-neuronal cells, and particularly astrocytes and microglia, make major contributions to the onset and progression of Alzheimer's disease

[61–63]. We add novel data to this growing body of evidence to demonstrate that interactions between the astrocytic chemokine CXCL1 and its neuronal receptor CXCR2 promote synaptotoxicity in the presence of A β . As such, our findings further elucidate non-cell autonomous mechanisms underlying synaptotoxic A β -tau interactions in AD. There is considerable regional heterogeneity of astrocytes, along with temporal alterations in astrocyte biology with aging and during disease [27, 64] and as such the precise contribution of reactive astrocytes to AD is not clearly established. Our work supports the assertion that rather than becoming reactive secondary to neuronal damage, at least some sub-types of astrocytes respond to AD-mimicking conditions during early “cellular phases” of disease.

Dendritic spines were used here as a measure of synapse health. These structures are post-synaptic sites for the majority of excitatory neurons [65]. Loss of spine density is linked with cognitive decline in humans and is a strong correlate of dementia in AD [1, 66, 67]. We examined dendritic spines in mouse neurons and also neuritic protrusions as a proxy for dendritic spines in human neurons that were differentiated from LUHMES. While LUHMES are a useful model for high throughput screening of changes in neuronal complexity and function [59], our data shows that their protrusion/spine density indicates that they are relatively immature, at least at the time in culture (DIV) examined here. Nevertheless, the changes we showed in the human neurons closely mimicked those we observed in murine primary neurons.

Importantly, reductions in spine density in AD are closely associated with abnormal tau, but less so with A β pathology [66], at least in the prefrontal cortex. However, particularly oligomeric forms of A β induce network excitability and synaptotoxicity *in vitro* and *in vivo* [68–71]. Together, these findings suggest that while A β may drive synaptic dysfunction in AD, tau is the executioner. Consistent with this assertion, together with a loss of dendritic spines upon exposure to TGCM astro we also see

(See figure on next page.)

Fig. 4 Astrocytic inflammatory phenotypes are induced by A β . To explore the effects of physiological A β concentrations on astrocyte phenotypes, a number of inflammatory markers were examined. **A** Representative images from mouse astrocytes exposed to TGCM for 24 h showed increased GFAP immunoreactivity (red) relative to those treated with WTCM. Scale bar = 100 μ m. Lysates from treated astrocytes were immunoblotted with antibodies against **B** GFAP, **C** phospho-NF κ B (p65) and **D** Lcn2. GAPDH was used as a loading control. Quantification of band intensities showed increases in **E** GFAP, **F** pNF κ B and **G** Lcn2 in TGCM-treated cultures relative to astrocytes treated with WTCM. Levels of the protein of interest were normalised to GAPDH in each case ($n = 5$, five independent cultures each containing three technical repeats). Data was quantified using unpaired *t* tests. Antibody-based cytokine arrays were used to provide unbiased analysis of cytokine content in medium from WTCM and TGCM exposed mouse and human astrocytes and in tissue homogenates from postmortem AD and control brain. Representative membranes showing increased CXCL1 in TGCM conditions are shown for **H** mouse astrocytes ($n = 4$, four independent experiments each performed in triplicate) and **J** human iNPC-astrocytes ($n = 3$, three independent experiments each performed in triplicate). **L** Total protein normalised cytosolic fractions of postmortem control and BA9 prefrontal cortex of AD brain at different Braak stages ($n = 4$ control, $n = 7$ stage I–II, $n = 10$ stage III–IV, $n = 6$ stage V–VI). Quantification of CXCL1 amounts in these samples revealed significant increases in CXCL1 in TGCM-treated **I** mouse and **K** human astrocytes, and **M** in Braak stage V–VI human AD brain. Data was analysed using *t* test or one-way ANOVA with Dunnett's post-hoc tests. Data on graphs is mean \pm SEM and is relative to control (control brain or WTCM). * $p < 0.05$

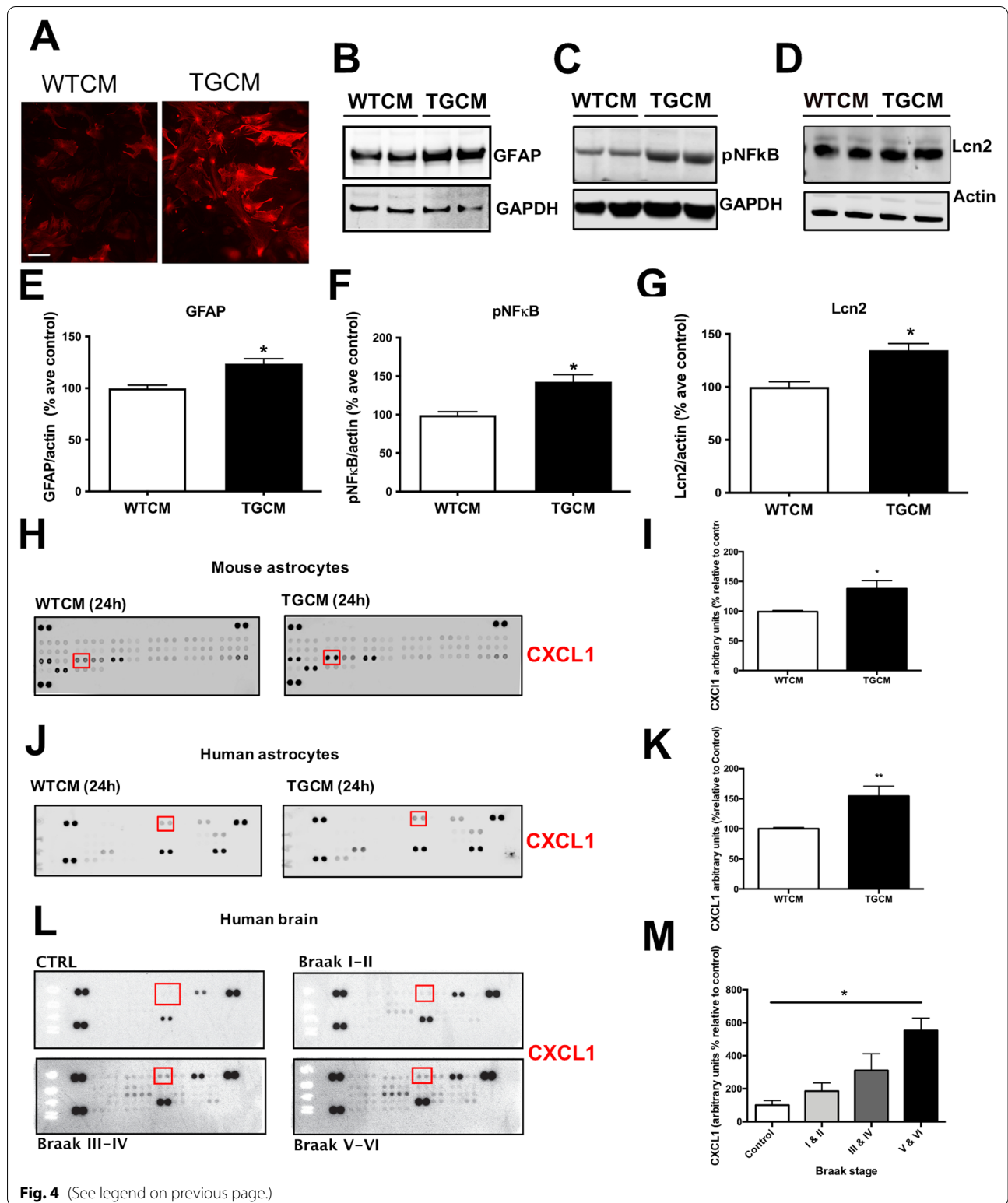
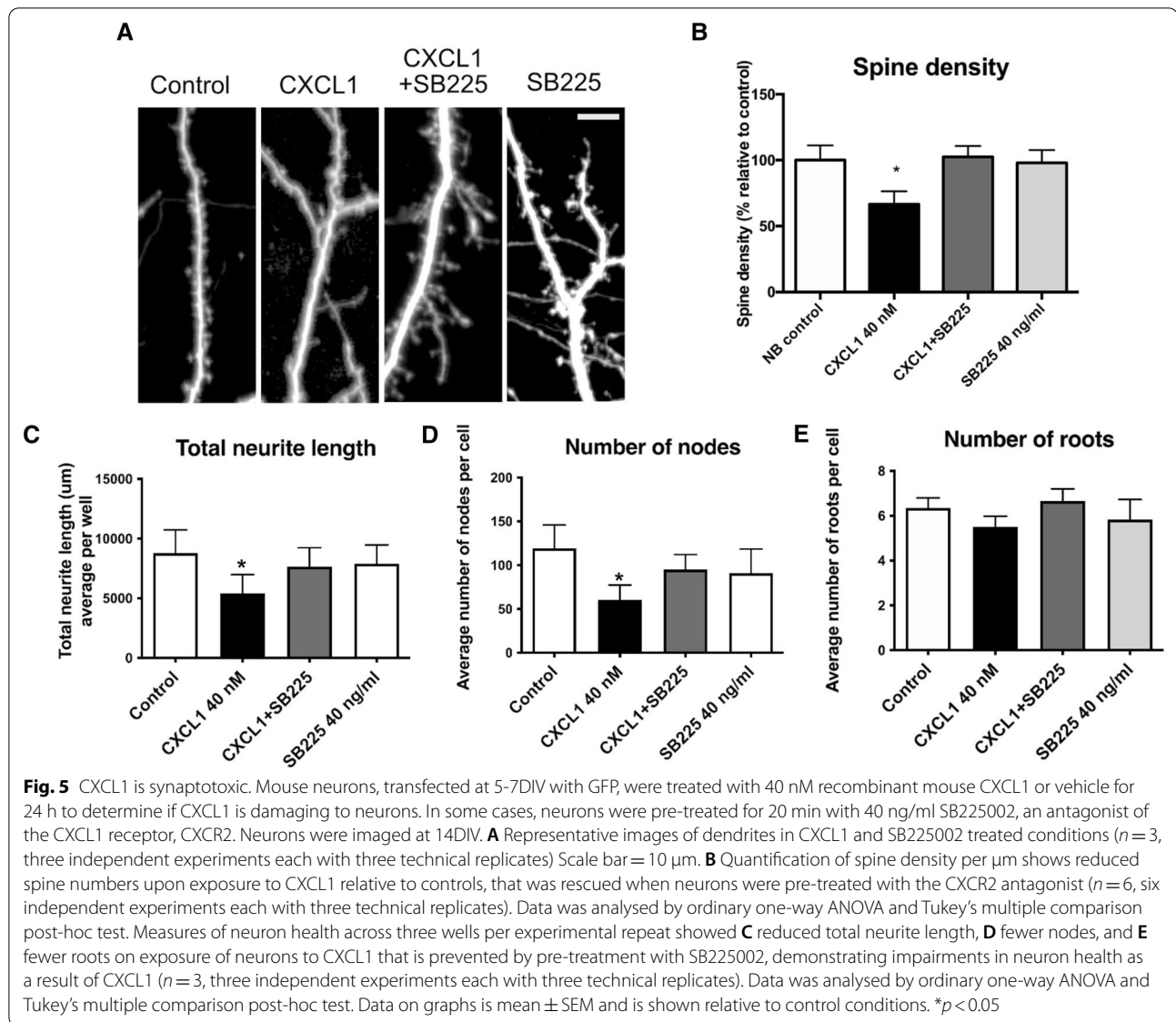


Fig. 4 (See legend on previous page.)

increased neuritic tau that might be indicative of the damaging mis-sorting of tau from the soma to synaptic compartments.

Tau mislocalisation from the cytoplasmic to synaptic fraction of AD brain is closely correlated with dementia in AD [15] and is a key pathological observation

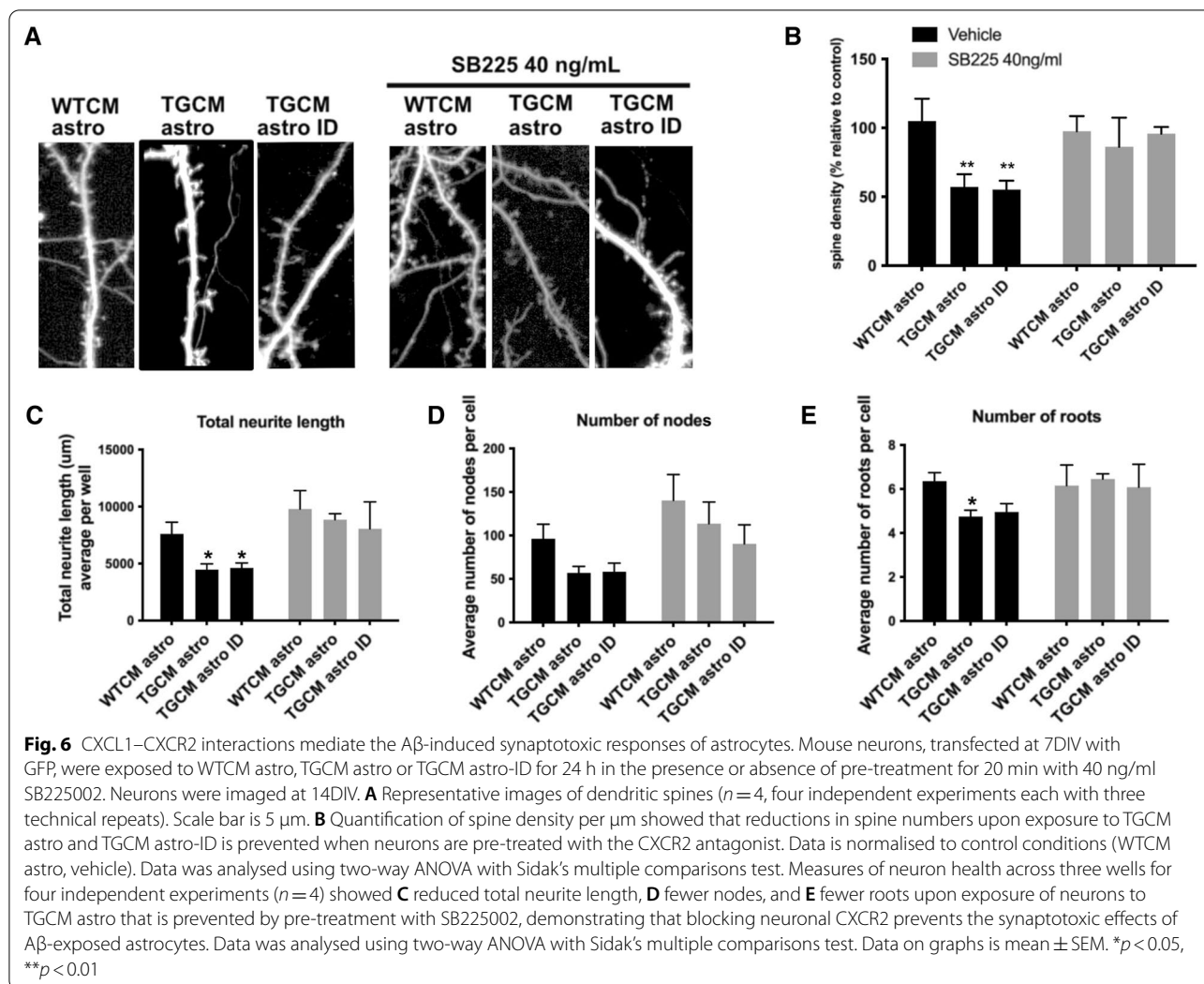


in tauopathy brain [72]. Although some tau is found in dendrites under physiological conditions [73, 74], dendritic tau is increased by $A\beta$, and can interact with post-synaptic components to further mediate excitotoxicity to $A\beta$ [11, 75]. We add to these findings by showing that in addition to having direct effects on neurons, secretions from $A\beta$ -stimulated astrocytes also induce tau mislocalisation and loss of dendritic spines.

"A1" astrocytes were defined by [30] following gene expression analysis from Zamanian et al. [38] as reactive astrocytes with neurotoxic properties. Neurons cultured with "A1" astrocytes, exhibit synaptotoxicity attributed to loss of physiological functions of astrocytes in synaptic maintenance and neuronal homeostasis, alongside secretion of at least one neurotoxic factor [30]. Recently, this

group identified saturated lipids contained in Apolipoprotein (APO)E and APOJ lipoparticles as mediators of astrocyte-induced toxicity [76], although it is important to note that this is context-dependent.

Our data show that astrocytes stimulated by $A\beta$, which is similar in concentration and species to that found in AD brain [42, 51, 52], increase their release of several cytokines, including the inflammatory chemokine CXCL1. Similar findings have been reported in mouse models of AD and prion disease, particularly following a secondary challenge [36]. We provide evidence that CXCL1 is likely one of the neurotoxic factors secreted by astrocytes, since direct application of recombinant CXCL1 recapitulated the loss of dendritic spines that occurs in response to whole conditioned medium from



Aβ-stimulated astrocytes (TGCM astro). Importantly, pharmacological blockade of the receptor for CXCL1, CXCR2, prevented both CXCL1- and TGCM astro-induced loss of dendritic spines.

CXCR2 is predominantly expressed in neurons, where it is upregulated proximal to amyloid plaques in AD brain [60]. Interestingly, CXCL1 has previously been shown to induce tau phosphorylation via downstream effects on ERK1/2 and PI-3 kinase [60]. CXCL1 also promotes caspase-3 activation [77]. Caspase-3 activity is increased by Aβ, it cleaves tau into pro-aggregatory fragments that seed neurofibrillary pathology [78] and is closely linked with synaptic disruption in AD [55]. Direct application of CXCL1 to long-term cultured neurons led to caspase-3 activation, caspase-3 mediated tau cleavage, and tau mislocalisation into bead-like varicosities along neuronal processes [77]. Our data, which show that treatment of neurons with TGCM astro, that contains increased levels of CXCL1, led to increased cleaved caspase-3 in

neurons and increased levels of neuritic tau, consistent with these previous reports. We speculate that caspase-3 mediated cleavage of tau might induce the mislocalisation of truncated tau into synaptic fractions to disrupt synapse health. It would be interesting to determine if blocking this tau truncation would protect synapses from Aβ-induced toxicity.

Conclusions

Our data show accelerated loss of dendritic spines upon interactions between CXCL1, secreted from reactive astrocytes in response to TGCM, and neuronal CXCR2 receptors. These data strongly support further investigation of the CXCL1–CXCR2 interaction in rodent models of AD with Aβ (and tau) abnormalities to determine if this ligand–receptor pair is a novel target for therapeutic intervention.

Abbreviations

A β : Beta-amyloid; AD: Alzheimer's disease; ATP: Adenosine triphosphate; APO (E/J): Apolipoprotein; BA: Brodmann area; BCA: Bicinchoninic acid; CCL2: C–C motif chemokine ligand 2; CXCL1: C–X–C motif chemokine ligand 1; CXCR2: CXC chemokine receptor 2; ERK: Extracellular signal related kinase; FGF: Fibroblast growth factor; GABA: Gamma-aminobutyric acid; GFAP: Glial fibrillary acidic protein; IL: Interleukin; IP-10: Interferon gamma-induced protein 10 (CXCL10); LUHMES: Lund human mesencephalic cells; MAP2: Microtubule associated protein 2; M-CSF: Monocyte colony stimulating factor; PI-3 kinase: Phosphoinositide 3-kinase; PSD-95: Postsynaptic density protein-95; TGCM: Conditioned medium from Tg2576 neurons; TGCM astro: Conditioned medium from astrocytes stimulated with TGCM; TGCM astro ID: Conditioned medium from astrocytes stimulated with TGCM and immunodepleted of A β ; TGCM h-astro: Conditioned medium from human astrocytes stimulated with TGCM; TGCM h-astro ID: Conditioned medium from human astrocytes stimulated with TGCM and immunodepleted of A β ; WTCM: Conditioned medium from wild-type neurons; WTCM astro: Conditioned medium from astrocytes stimulated with WTCM; WTCM astro: Conditioned medium from astrocytes stimulated with WTCM; WTCM h-astro: Conditioned medium from human astrocytes stimulated with WTCM.

Supplementary Information

The online version contains supplementary material available at <https://doi.org/10.1186/s12974-021-02371-0>.

Additional file 1: Figure S1. Immunodepletion of A β from astrocyte medium with 6E10. **Figure S2.** Measures of neuronal health and complexity in mouse neurons challenged with WTCM astro, TGCM astro and TGCM astro-ID. **Figure S3.** Measures of neuronal health and complexity in LUHMES challenged with WTCM h-astro, TGCM h-astro and TGCM h-astro-ID. **Figure S4.** Immunofluorescence of tau relative to MAP2 in neurons exposed to CXCL1.

Acknowledgements

We thank Dr George Chennell at the Wohl Cellular Imaging Centre at King's College London for help with microscopy, Professor Dame Pamela Shaw (Sheffield Institute of Translational Neuroscience) for access to fibroblasts from non-ALS controls, and the sadly missed Professor Peter Davies (Feinstein Institute of Medical Research, NY) for the kind gift of tau antibodies.

Author contributions

BGP-N and WN designed the study. BGP-N and WN wrote the manuscript. BGP-N performed most experiments and analysed data. LJ, PBL, MMH, LG, FT, MAM, IV-V, MJS, CT, SBW and LF performed additional experiments and/or data analysis and/or contributed to study design. All authors edited and approved the manuscript. All authors read and approved the final manuscript.

Funding

This work was supported by Alzheimer's Research UK (King's College London ARUK Network Centre, ARUK-RF2014-2 to BGP-N, ARUK-EG2013-B1 to WN, ARUK-PhD2018-002 to WN and BGP-N, PG2019A-003 to SBW), the Van Geest Charitable Trust (to BGP-N), a grant from Consejo Nacional de Ciencia y Tecnología (CONACYT), Mexico (to IV), a Career Development Award from the Medical Research Council (MR/N022696/1 to MJ-S) and grants from the Thierry Latran Foundation and the Academy of Medical Sciences (Ref: SBF002/1142 to LF). Human tissue samples were provided by the London Neurodegenerative Diseases Brain Bank, which receives funding from the MRC and through the Brains for Dementia Research programme (jointly funded by Alzheimer's Society and Alzheimer's Research UK).

Availability of data and materials

Summary data are available from the authors on request.

Declarations

Ethics approval consent to participate

All animal work was conducted in accordance with the UK Animals (Scientific Procedures) Act 1986 and the European Directive 2010/63/EU under UK Home Office Personal and Project Licenses and with agreement from the King's College London (Denmark Hill) Animal Welfare and Ethical Review Board. All thuman issue collection and processing were carried out under the regulations and licensing of the Human Tissue Authority, and in accordance with the UK Human Tissue Act, 2004. All skin biopsy donors provided informed consent before sample collection (University of Sheffield, Study number STH16573, Research Committee reference 12/YH/0330).

Consent for publication

Not applicable.

Competing interests

The authors declare that they have no competing interests.

Author details

¹Department of Basic and Clinical Neuroscience, Maurice Wohl Clinical Neuroscience Institute, Institute of Psychiatry, Psychology and Neuroscience, King's College London, 5 Cutcombe Road, London SE5 9RX, UK. ²Sheffield Institute for Translational Neuroscience (SITraN), University of Sheffield, Sheffield S10 2HQ, UK.

Received: 15 October 2021 Accepted: 22 December 2021

Published online: 28 December 2021

References

- DeKosky ST, Scheff SW. Synapse loss in frontal cortex biopsies in Alzheimer's disease: correlation with cognitive severity. *Ann Neurol*. 1990;27(5):457–64.
- Crimins JL, Pooler A, Polydoro M, Luebke JI, Spiess-Jones TL. The intersection of amyloid beta and tau in glutamatergic synaptic dysfunction and collapse in Alzheimer's disease. *Ageing Res Rev*. 2013;12(3):757–63.
- Bertoni-Freddari C, Fattoretti P, Paoloni R, Caselli U, Galeazzi L, Meier-Ruge W. Synaptic structural dynamics and aging. *Gerontology*. 1996;42(3):170–80.
- Colom-Cadena M, Spiess-Jones T, Zetterberg H, Blennow K, Caggiano A, DeKosky ST, et al. The clinical promise of biomarkers of synapse damage or loss in Alzheimer's disease. *Alzheimers Res Ther*. 2020;12(1):21.
- Cleary JP, Walsh DM, Hofmeister JJ, Shankar GM, Kuskowski MA, Selkoe DJ, et al. Natural oligomers of the amyloid-beta protein specifically disrupt cognitive function. *Nat Neurosci*. 2005;8(1):79–84.
- Walsh DM, Klyubin I, Fadeeva JV, Cullen WK, Anwyl R, Wolfe MS, et al. Naturally secreted oligomers of amyloid beta protein potently inhibit hippocampal long-term potentiation in vivo. *Nature*. 2002;416(6880):535–9.
- Walsh DM, Townsend M, Podlisky MB, Shankar GM, Fadeeva JV, El Agnaf O, et al. Certain inhibitors of synthetic amyloid beta-peptide (A β) fibrillogenesis block oligomerization of natural A β and thereby rescue long-term potentiation. *J Neurosci*. 2005;25(10):2455–62.
- Shankar GM, Bloodgood BL, Townsend M, Walsh DM, Selkoe DJ, Sabatini BL. Natural oligomers of the Alzheimer amyloid-beta protein induce reversible synapse loss by modulating an NMDA-type glutamate receptor-dependent signaling pathway. *J Neurosci*. 2007;27(11):2866–75.
- Shankar GM, Li S, Mehta TH, Garcia-Munoz A, Shepardson NE, Smith I, et al. Amyloid-beta protein dimers isolated directly from Alzheimer's brains impair synaptic plasticity and memory. *Nat Med*. 2008;14(8):837–42.
- Walsh S, Merrick R, Milne R, Brayne C. Aducanumab for Alzheimer's disease? *BMJ*. 2021;374:n1682.
- Ittner LM, Ke YD, Delerue F, Bi M, Gladbach A, van Eersel J, et al. Dendritic function of tau mediates amyloid-beta toxicity in Alzheimer's disease mouse models. *Cell*. 2010;142(3):387–97.
- Hoover BR, Reed MN, Su J, Penrod RD, Kotilinek LA, Grant MK, et al. Tau mislocalization to dendritic spines mediates synaptic dysfunction independently of neurodegeneration. *Neuron*. 2010;68(6):1067–81.

13. Zhou L, McInnes J, Wierda K, Holt M, Herrmann AG, Jackson RJ, et al. Tau association with synaptic vesicles causes presynaptic dysfunction. *Nat Commun.* 2017;8:15295.
14. McInnes J, Wierda K, Snellinx A, Bounti L, Wang YC, Stancu IC, et al. Synaptogyrin-3 mediates presynaptic dysfunction induced by Tau. *Neuron.* 2018;97(4):823–35.
15. Perez-Nievas BG, Stein TD, Tai HC, Dols-Icardo O, Scotton TC, Barroeta-Espar I, et al. Dissecting phenotypic traits linked to human resilience to Alzheimer's pathology. *Brain.* 2013;136(Pt 8):2510–26.
16. Augusto-Oliveira M, Arrifano GP, Takeda PY, Lopes-Araujo A, Santos-Sacramento L, Anthony DC, et al. Astroglia-specific contributions to the regulation of synapses, cognition and behaviour. *Neurosci Biobehav Rev.* 2020;118:331–57.
17. Parpura V, Basarsky TA, Liu F, Jęftinija K, Jęftinija S, Haydon PG. Glutamate-mediated astrocyte-neuron signalling. *Nature.* 1994;369(6483):744–7.
18. Parpura V, Verkhratsky A. The astrocyte excitability brief: from receptors to gliotransmission. *Neurochem Int.* 2012;61(4):610–21.
19. Verkhratsky A, Parpura V, Vardjan N, Zorec R. Physiology of Astroglia. *Adv Exp Med Biol.* 2019;1175:45–91.
20. Volterra A, Meldolesi J. Astrocytes, from brain glue to communication elements: the revolution continues. *Nat Rev Neurosci.* 2005;6(8):626–40.
21. Santello M, Toni N, Volterra A. Astrocyte function from information processing to cognition and cognitive impairment. *Nat Neurosci.* 2019;22(2):154–66.
22. Mederos S, Gonzalez-Arias C, Perea G. Astrocyte-neuron networks: a multilane highway of signaling for homeostatic brain function. *Front Synaptic Neurosci.* 2018;10:45.
23. Lushnikova I, Skibo G, Muller D, Nikonenko I. Synaptic potentiation induces increased glial coverage of excitatory synapses in CA1 hippocampus. *Hippocampus.* 2009;19(8):753–62.
24. Itagaki S, McGeer PL, Akiyama H, Zhu S, Selkoe D. Relationship of microglia and astrocytes to amyloid deposits of Alzheimer disease. *J Neuroimmunol.* 1989;24(3):173–82.
25. Perez-Nievas BG, Serrano-Pozo A. Deciphering the astrocyte reaction in Alzheimer's disease. *Front Aging Neurosci.* 2018;10:114.
26. Serrano-Pozo A, Frosch MP, Masliah E, Hyman BT. Neuropathological alterations in Alzheimer disease. *Cold Spring Harb Perspect Med.* 2011;1(1):a006189.
27. Escartin C, Galea E, Lakatos A, O'Callaghan JP, Petzold GC, Serrano-Pozo A, et al. Reactive astrocyte nomenclature, definitions, and future directions. *Nat Neurosci.* 2021;24(3):312–25.
28. Bellaver B, Ferrari-Souza JP, Uglione da Ros L, Carter SF, Rodriguez-Vieitez E, Nordberg A, et al. Astrocyte biomarkers in Alzheimer disease: a systematic review and meta-analysis. *Neurology.* 2021. <https://doi.org/10.1212/WNL.00000000000012109>.
29. Elahi FM, Casaletto KB, La Joie R, Walters SM, Harvey D, Wolf A, et al. Plasma biomarkers of astrocytic and neuronal dysfunction in early- and late-onset Alzheimer's disease. *Alzheimers Dement.* 2020;16(4):681–95.
30. Liddelow SA, Guttenplan KA, Clarke LE, Bennett FC, Bohlen CJ, Schirmer L, et al. Neurotoxic reactive astrocytes are induced by activated microglia. *Nature.* 2017;541(7638):481–7.
31. Bhat R, Crowe EP, Bitto A, Moh M, Katsetos CD, Garcia FU, et al. Astrocyte senescence as a component of Alzheimer's disease. *PLoS ONE.* 2012;7(9):e45069.
32. Garwood CJ, Pooler AM, Atherton J, Hanger DP, Noble W. Astrocytes are important mediators of Abeta-induced neurotoxicity and tau phosphorylation in primary culture. *Cell Death Dis.* 2011;2:e167.
33. Lian H, Litvinchuk A, Chiang AC, Aithmitti N, Jankowsky JL, Zheng H. Astrocyte-microglia cross talk through complement activation modulates amyloid pathology in mouse models of Alzheimer's disease. *J Neurosci.* 2016;36(2):577–89.
34. Staurengi E, Cerrato V, Gamba P, Testa G, Giannelli S, Leoni V, et al. Oxysterols present in Alzheimer's disease brain induce synaptotoxicity by activating astrocytes: a major role for lipocalin-2. *Redox Biol.* 2021;39:101837.
35. Cunningham C, Dunne A, Lopez-Rodriguez AB. Astrocytes: heterogeneous and dynamic phenotypes in neurodegeneration and innate immunity. *Neuroscientist.* 2019;25(5):455–74.
36. Lopez-Rodriguez AB, Hennessy E, Murray CL, Nazmi A, Delaney HJ, Healy D, et al. Acute systemic inflammation exacerbates neuroinflammation in Alzheimer's disease: IL-1beta drives amplified responses in primed astrocytes and neuronal network dysfunction. *Alzheimers Dement.* 2021;17(10):1735–55.
37. McAlpine CS, Park J, Griciuc A, Kim E, Choi SH, Iwamoto Y, et al. Astrocytic interleukin-3 programs microglia and limits Alzheimer's disease. *Nature.* 2021;595(7869):701–6.
38. Zamanian JL, Xu L, Foo LC, Nouri N, Zhou L, Giffard RG, et al. Genomic analysis of reactive astrogliosis. *J Neurosci.* 2012;32(18):6391–410.
39. Zeisel A, Hochgerner H, Lonnerberg P, Johansson A, Memic F, van der Zwan J, et al. Molecular architecture of the mouse nervous system. *Cell.* 2018;174(4):999–1014.
40. Hsiao K, Chapman P, Nilsen S, Eckman C, Harigaya Y, Younkin S, et al. Correlative memory deficits, Abeta elevation, and amyloid plaques in transgenic mice. *Science.* 1996;274(5284):99–102.
41. Mitchell JC, Ariff BB, Yates DM, Lau KF, Perkinson MS, Rogelj B, et al. X11beta rescues memory and long-term potentiation deficits in Alzheimer's disease APPswe Tg2576 mice. *Hum Mol Genet.* 2009;18(23):4492–500.
42. Hudry E, Wu HY, Arbel-Ornath M, Hashimoto T, Matsouka R, Fan Z, et al. Inhibition of the NFAT pathway alleviates amyloid beta neurotoxicity in a mouse model of Alzheimer's disease. *J Neurosci.* 2012;32(9):3176–92.
43. Arbel-Ornath M, Hudry E, Boivin JR, Hashimoto T, Takeda S, Kuchibhotla KV, et al. Soluble oligomeric amyloid-beta induces calcium dyshomeostasis that precedes synapse loss in the living mouse brain. *Mol Neurodegener.* 2017;12(1):27.
44. Schildge S, Bohrer C, Beck K, Schachtrup C. Isolation and culture of mouse cortical astrocytes. *J Vis Exp.* 2013;(71):50079.
45. Meyer K, Ferraiuolo L, Miranda CJ, Likhite S, McElroy S, Renuch S, et al. Direct conversion of patient fibroblasts demonstrates non-cell autonomous toxicity of astrocytes to motor neurons in familial and sporadic ALS. *Proc Natl Acad Sci U S A.* 2014;111(2):829–32.
46. Allen SP, Hall B, Castelli LM, Francis L, Woof R, Siskos AP, et al. Astrocyte adenosine deaminase loss increases motor neuron toxicity in amyotrophic lateral sclerosis. *Brain.* 2019;142(3):586–605.
47. Varianna A, Myszczyńska MA, Castelli LM, O'Neill B, Kim Y, Talbot J, et al. Micro-RNAs secreted through astrocyte-derived extracellular vesicles cause neuronal network degeneration in C9orf72 ALS. *EBioMedicine.* 2019;40:626–35.
48. Ratcliffe LE, Vazquez Villaseñor I, Jennings L, Heath PR, Mortiboys H, Schwartzentruber A, et al. Loss of IGF1R in human astrocytes alters complex I activity and support for neurons. *Neuroscience.* 2018;390:46–59.
49. Croft CL, Noble W. Preparation of organotypic brain slice cultures for the study of Alzheimer's disease. *F1000Res.* 2018;7:592.
50. Wu HY, Hudry E, Hashimoto T, Kuchibhotla K, Rozkalne A, Fan Z, et al. Amyloid beta induces the morphological neurodegenerative triad of spine loss, dendritic simplification, and neuritic dystrophies through calcineurin activation. *J Neurosci.* 2010;30(7):2636–49.
51. DaRocha-Souto B, Coma M, Perez-Nievas BG, Scotton TC, Siao M, Sanchez-Ferrer P, et al. Activation of glycogen synthase kinase-3 beta mediates beta-amyloid induced neuritic damage in Alzheimer's disease. *Neurobiol Dis.* 2012;45(1):425–37.
52. Wu HY, Hudry E, Hashimoto T, Uemura K, Fan ZY, Berezovska O, et al. Distinct dendritic spine and nuclear phases of calcineurin activation after exposure to amyloid-beta revealed by a novel fluorescence resonance energy transfer assay. *J Neurosci.* 2012;32(15):5298–309.
53. Glennon EB, Lau DH, Gabriele RMC, Taylor MF, Troakes C, Opie-Martin S, et al. Bridging Integrator-1 protein loss in Alzheimer's disease promotes synaptic tau accumulation and disrupts tau release. *Brain Commun.* 2020;2(1):fcaa011.
54. Srivastava DP, Woolfrey KM, Penzes P. Analysis of dendritic spine morphology in cultured CNS neurons. *J Vis Exp.* 2011;53:e2794.
55. D'Amelio M, Sheng M, Ceconi F. Caspase-3 in the central nervous system: beyond apoptosis. *Trends Neurosci.* 2012;35(11):700–9.
56. Li J, Pan L, Pembroke WG, Rexach JE, Godoy MI, Condro MC, et al. Conservation and divergence of vulnerability and responses to stressors between human and mouse astrocytes. *Nat Commun.* 2021;12(1):3958.
57. Gatto N, Dos Santos SC, Shaw AC, Bell SM, Myszczyńska MA, Powers S, et al. Directly converted astrocytes retain the ageing features of the donor fibroblasts and elucidate the astrocytic contribution to human CNS health and disease. *Aging Cell.* 2021;20(1):e13281.

58. Scholz D, Polt D, Genewsky A, Weng M, Waldmann T, Schildknecht S, et al. Rapid, complete and large-scale generation of post-mitotic neurons from the human LUHMES cell line. *J Neurochem*. 2011;119(5):957–71.
59. Leah T, Vazquez-Villasenor I, Ferraiuolo L, Wharton SB, Mortiboys H. A Parkinson's disease-relevant mitochondrial and neuronal morphology high-throughput screening assay in LUHMES cells. *Bio Protoc*. 2021;11(1):e3881.
60. Xia M, Hyman BT. GROalpha/KC, a chemokine receptor CXCR2 ligand, can be a potent trigger for neuronal ERK1/2 and PI-3 kinase pathways and for tau hyperphosphorylation—a role in Alzheimer's disease? *J Neuroimmunol*. 2002;122(1–2):55–64.
61. Henstridge CM, Hyman BT, Spires-Jones TL. Beyond the neuron-cellular interactions early in Alzheimer disease pathogenesis. *Nat Rev Neurosci*. 2019;20(2):94–108.
62. Scheltens P, De Strooper B, Kivipelto M, Holstege H, Chetelat G, Teunissen CE, et al. Alzheimer's disease. *Lancet*. 2021;397(10284):1577–90.
63. Paumier A, Boisseau S, Jacquier-Sarlin M, Pernet-Gallay K, Buisson A, Albrieux M. Astrocyte-neuron interplay is critical for Alzheimer's disease pathogenesis and is rescued by TRPA1 channel blockade. *Brain*. 2021. <https://doi.org/10.1093/brain/awab281>.
64. Boisvert MM, Erikson GA, Shokhirev MN, Allen NJ. The aging astrocyte transcriptome from multiple regions of the mouse brain. *Cell Rep*. 2018;22(1):269–85.
65. Walker CK, Herskowitz JH. Dendritic spines: mediators of cognitive resilience in aging and Alzheimer's disease. *Neuroscientist*. 2021;27(5):487–505.
66. Boros BD, Greathouse KM, Gentry EG, Curtis KA, Birchall EL, Gearing M, et al. Dendritic spines provide cognitive resilience against Alzheimer's disease. *Ann Neurol*. 2017;82(4):602–14.
67. Chen MK, Mecca AP, Naganawa M, Finnema SJ, Toyonaga T, Lin SF, et al. Assessing synaptic density in Alzheimer disease with synaptic vesicle glycoprotein 2A positron emission tomographic imaging. *JAMA Neurol*. 2018;75(10):1215–24.
68. Blurton-Jones M, Laferla FM. Pathways by which Abeta facilitates tau pathology. *Curr Alzheimer Res*. 2006;3(5):437–48.
69. Ittner LM, Gotz J. Amyloid-beta and tau—a toxic pas de deux in Alzheimer's disease. *Nat Rev Neurosci*. 2011;12(2):65–72.
70. Mucke L, Selkoe DJ. Neurotoxicity of amyloid beta-protein: synaptic and network dysfunction. *Cold Spring Harb Perspect Med*. 2012;2(7):a006338.
71. Siskova Z, Justus D, Kaneko H, Friedrichs D, Henneberg N, Beutel T, et al. Dendritic structural degeneration is functionally linked to cellular hyperexcitability in a mouse model of Alzheimer's disease. *Neuron*. 2014;84(5):1023–33.
72. Braak H, Thal DR, Ghebremedhin E, Del Tredici K. Stages of the pathologic process in Alzheimer disease: age categories from 1 to 100 years. *J Neuro-pathol Exp Neurol*. 2011;70(11):960–9.
73. Ittner A, Ittner LM. Dendritic Tau in Alzheimer's disease. *Neuron*. 2018;99(1):13–27.
74. Xia D, Gutmann JM, Gotz J. Mobility and subcellular localization of endogenous, gene-edited Tau differs from that of over-expressed human wild-type and P301L mutant Tau. *Sci Rep*. 2016;6:29074.
75. Li C, Gotz J. Somatodendritic accumulation of Tau in Alzheimer's disease is promoted by Fyn-mediated local protein translation. *EMBO J*. 2017;36(21):3120–38.
76. Guttenplan KA, Weigel MK, Prakash P, Wijewardhane PR, Hasel P, Rufen-Blanchette U, et al. Neurotoxic reactive astrocytes induce cell death via saturated lipids. *Nature*. 2021;599:102.
77. Zhang XF, Zhao YF, Zhu SW, Huang WJ, Luo Y, Chen QY, et al. CXCL1 triggers caspase-3 dependent tau cleavage in long-term neuronal cultures and in the hippocampus of aged mice: implications in Alzheimer's disease. *J Alzheimers Dis*. 2015;48(1):89–104.
78. Cotman CW, Poon WW, Rissman RA, Blurton-Jones M. The role of caspase cleavage of tau in Alzheimer disease neuropathology. *J Neuropathol Exp Neurol*. 2005;64(2):104–12.

Publisher's Note

Springer Nature remains neutral with regard to jurisdictional claims in published maps and institutional affiliations.

Ready to submit your research? Choose BMC and benefit from:

- fast, convenient online submission
- thorough peer review by experienced researchers in your field
- rapid publication on acceptance
- support for research data, including large and complex data types
- gold Open Access which fosters wider collaboration and increased citations
- maximum visibility for your research: over 100M website views per year

At BMC, research is always in progress.

Learn more biomedcentral.com/submissions

